Potent Lectin-Independent Chaperone Function of Calnexin under Conditions Prevalent within the Lumen of the Endoplasmic Reticulum†

Achim Brockmeier and David B. Williams*

Departments of Biochemistry and Immunology, University of Toronto, Toronto, Ontario, Canada M5S 1A8

Received July 16, 2006; Revised Manuscript Received August 28, 2006

ABSTRACT: Calnexin is a membrane-bound chaperone of the endoplasmic reticulum (ER) that participates in the folding and quality control of newly synthesized glycoproteins. Binding to glycoproteins occurs through a lectin site with specificity for $Glc_1Man_9GlcNAc_2$ oligosaccharides as well as through a polypeptide binding site that recognizes non-native protein conformations. The latter interaction is somewhat controversial because it is based on observations that calnexin can suppress the aggregation of non-glycosylated substrates at elevated temperature or at low calcium concentrations, conditions that may affect the structural integrity of calnexin. Here, we examine the ability of calnexin to interact with a non-glycosylated substrate under physiological conditions of the ER lumen. We show that the soluble ER luminal domain of calnexin can indeed suppress the aggregation of non-glycosylated firefly luciferase at 37 °C and at the normal resting ER calcium concentration of 0.4 mM. However, gradual reduction of calcium below the resting level was accompanied by a progressive loss of native calnexin structure as assessed by thermal stability, protease sensitivity, intrinsic fluorescence, and bis-ANS binding. These assays permitted the characterization of a single calcium binding site on calnexin with a $K_d = 0.15 \pm 0.05$ mM. We also show that the suppression of firefly luciferase aggregation by calnexin is strongly enhanced in the presence of millimolar concentrations of ATP and that the K_d for ATP binding to calnexin in the presence of 0.4 mM calcium is 0.7 mM. ATP did not alter the overall stability of calnexin but instead triggered the localized exposure of a hydrophobic site on the chaperone. These findings demonstrate that calnexin is a potent molecular chaperone that is capable of suppressing the aggregation of substrates through polypeptide-based interactions under conditions that exist within the ER lumen.

The endoplasmic reticulum (ER)[1] membrane protein calnexin (Cnx) and its soluble homologue calreticulin (Crt) are components of a chaperone system that assists in the folding of Asn-linked glycoproteins. These chaperones also participate in quality control, retaining non-native glycoproteins within the ER either until a native conformation is achieved or until they are degraded by the ER-associated degradation (ERAD) machinery (*1*−*3*). The ER luminal portion of Cnx consists of two domains, a globular lectin domain and an extended hairpin-like arm domain (*4*). The lectin domain recognizes an early oligosaccharide processing intermediate on folding glycoproteins, $Glc_1Man_9GlcNAc_2$ (*5*, *6*), whereas the tip of the arm domain provides a binding site for ERp57, a thiol oxidoreductase of the protein disulfide isomerase family (*5*, *7*). Crt possesses an ERp57-binding arm domain (*8*) and is presumed to contain a Cnx-like globular domain because it shares identical lectin specificity with Cnx (*9*, *10*). Both chaperones also bind calcium, which is required for their lectin function (*10*).

As a nascent glycoprotein enters the ER lumen, it is co-translationally glycosylated with a preassembled $Glc_3Man_9GlcNAc_2$ oligosaccharide, which is rapidly processed by glucosidases I and II to the $Glc_1Man_9GlcNAc_2$ species that is recognized by Cnx and Crt. Cycles of chaperone binding and release are then thought to be controlled by the availability of the terminal glucose on the $Glc_1Man_9GlcNAc_2$ oligosaccharide (*11*, *12*). Release occurs in conjunction with the removal of the terminal glucose by glucosidase II, at which point the glycoprotein may fold and be exported from the ER. However, if folding does not occur promptly, the glycoprotein becomes a substrate for UDP-glucose/glycoprotein glucosyltransferase (UGGT), an enzyme that reattaches the glucose residue only on non-native glycoprotein conformers (*13*−*15*). In this model, Cnx and Crt do not function as classical chaperones that prevent aggregation by binding to hydrophobic segments on glycoprotein folding intermediates. Rather they promote oxidative folding by recruiting ERp57 and possibly other folding enzymes to the vicinity of the folding glycoprotein (*16*). In the case of misfolded or mutant glycoproteins, extended cycles of binding and release contribute to retention within the ER and ultimately to ERAD (*17*−*20*).

† This work was supported by a grant from the Canadian Institutes of Health Research (to D.B.W.).

* To whom correspondence should be addressed. Tel: (416) 978-2546. Fax: (416) 978-8548. E-mail: david.williams@utoronto.ca.

[1] Abbreviations: bis-ANS, 1,1′-bis(4-anilino)naphthalene-5,5′-disulfonic acid; CD, circular dichroism; Cnx, calnexin; Crt, calreticulin; ER, endoplasmic reticulum; ERAD, ER-associated degradation; FL, firefly luciferase; GST, glutathione S-transferase; S-Cnx, soluble luminal domain of calnexin; UGGT, UDP-glucose/glycoprotein glucosyltransferase.

10.1021/bi0614378 CCC: $33.50
Published on Web 09/29/2006

In addition to their lectin and ERp57 binding sites, Cnx and Crt have been shown to be capable of suppressing the aggregation in vitro of either non-glycosylated protein substrates (*21*, *22*) or glycoproteins that lack monoglucosylated oligosaccharides (*23*, *24*), suggesting the presence of a polypeptide binding site similar to that of classical molecular chaperones. Furthermore, Cnx and Crt bind preferentially to non-native conformers of non-glycosylated proteins and exhibit enhanced capacity to suppress aggregation in the presence of ATP (*21*, *22*). These studies have led to the suggestion that Cnx and Crt utilize both lectin- and polypeptide-based modes of binding in their interactions with glycoprotein folding intermediates in the ER. In this dual-binding model, these chaperones promote folding by suppressing nonproductive aggregation reactions as well as through the recruitment of ERp57 to glycoprotein folding intermediates (*3*).

Because most of the in vitro aggregation suppression assays with Cnx and Crt were performed at elevated temperature (42−47 °C) to induce aggregation of the substrate (*21*−*24*) or involved the removal of Ca^{2+} (*23*, *24*), the possibility exists that polypeptide-based interactions are a consequence of an altered chaperone conformation that may not be prevalent under physiological conditions of the ER lumen. Consistent with such a possibility is the finding that Crt has a remarkably low melting temperature of 46.4 °C in buffer containing 1 mM Ca^{2+} (*25*). Consequently, we sought to determine whether aggregation suppression by these chaperones could be demonstrated at 37 °C and what influence physiological concentrations of Ca^{2+} and ATP may have on the process. Using an assay system that monitors aggregation of the non-glycosylated protein firefly luciferase (FL) at 37 °C, we show that the soluble ER luminal domain of Cnx (S-Cnx) is capable of suppressing FL aggregation at Ca^{2+} concentrations that are prevalent in the resting ER (0.3−0.5 mM) (*26*). Furthermore, the presence of millimolar concentrations of ATP profoundly enhance the aggregation suppression capability of S-Cnx. Biophysical characterization of the effects of ATP on the conformation of S-Cnx suggests the existence of an ATP-regulated hydrophobic binding site through which potent aggregation suppression is accomplished.

EXPERIMENTAL PROCEDURES

Purification of Soluble Cnx (S-Cnx). The bacterial expression vector pGEX-3X (GE Healthcare), encoding glutathione S-transferase fused to the N-terminus of the ER luminal domain of canine Cnx followed by a His_6 sequence (GST-Cnx; ref 21 (*21*)), was transformed into the *Escherichia coli* strain FA113, which possesses an oxidizing cytosol (*27*). Expression of the GST-Cnx fusion protein was induced with 1 mM isopropylthio-β-D-galactopyranoside for 16 h at room temperature (RT). Cells were harvested, resuspended in 50 mM Tris at pH 8, 300 mM NaCl, and 3 mM $CaCl_2$ and lysed by French Press at 4 °C. The fusion protein was then purified by nickel-agarose chromatography (Qiagen) according to the manufacturer's protocol (final elution with 250 mM imidazole). The eluate was dialyzed against 50 mM Tris at pH 8, 150 mM NaCl, and 1 mM $CaCl_2$ before the addition of (1 unit/mL) Factor Xa (GE Healthcare) to release S-Cnx from GST. After a 16 h digestion at RT, the $CaCl_2$ concentration was increased to 3 mM, and the digest was passed through a glutathione-agarose column (Sigma) to remove GST. The S-Cnx-containing flow-through fraction was dialyzed against 20 mM Tris at pH 8, 50 mM NaCl, and 3 mM $CaCl_2$, and S-Cnx was further purified by Mono Q anion exchange FPLC (8 mL column) (Pharmacia Biotech) using a linear, 200 mL 0.05−1 M NaCl gradient in 20 mM Tris at pH 8 and 3 mM $CaCl_2$. S-Cnx eluted typically at 0.43 M NaCl. From 2 L of bacterial culture, about 7 mg of S-Cnx could be obtained with a purity in excess of 95%. Purified S-Cnx was dialyzed against 20 mM Hepes at pH 7.4, 150 mM NaCl, and 1 mM $CaCl_2$ and frozen in aliquots at −20 °C. Aliquots were thawed only once, immediately prior to use.

Adjustment of Ca^{2+} Concentration. All experiments were performed using buffer consisting of 20 mM Hepes at pH 7.4, 150 mM NaCl, and 1 mM $CaCl_2$, with various protein or nucleotide additives being prepared in the same buffer. For experiments involving a fixed 1 mM Ca^{2+} concentration (Figures 4 and 5), all assay components were simply mixed together. For final Ca^{2+} concentrations other than 1 mM, adjustments were made using two methods. In the first method (Figures 1−3), samples were prepared by first adding buffer, followed by EDTA to a final concentration of 1 mM and then sufficient $CaCl_2$ to achieve the desired final free Ca^{2+} concentration. S-Cnx, firefly luciferase (FL), or other components were added last. The calcium contributed by these final additions was taken into account when calculating the final Ca^{2+} concentration. In the second method (Figure 6), S-Cnx and nucleotide (in 20 mM Hepes at pH 7.4, 150 mM NaCl, and 1 mM $CaCl_2$) were mixed with the appropriate amounts of $CaCl_2$ and calcium-free buffer (20 mM Hepes and 150 mM NaCl at pH 7.4) to achieve the desired final Ca^{2+} concentration. Final free Ca^{2+} concentrations were confirmed by direct measurement using the Ca^{2+}-specific electrode in a Radiometer ABL700 Blood Gas Analyzer (Radiometer, Copenhagen, Denmark). S-Cnx was typically equilibrated for 1 h in the final buffer prior to experiment, although preincubations as short as 10 min were sufficient.

Trypsin Digestion of S-Cnx. S-Cnx (48 μg) was preincubated in 20 mM Hepes, 150 mM NaCl at pH 7.4, and the indicated Ca^{2+} concentrations for 1 h at RT. All digestions were performed in a final volume of 360 μL at 37 °C with 0.48 μg of bovine pancreatic trypsin (type III-S, Sigma). Aliquots containing 4 μg of S-Cnx were removed at each time point, mixed with SDS−PAGE sample buffer, and heated at 95 °C for 5 min. Digestion products were analyzed by SDS−PAGE using 10% polyacrylamide gels with visualization by Coomassie Blue staining.

Aggregation Assay. Recombinant firefly luciferase (FL, Promega) was dialyzed against 20 mM Hepes at pH 7.4, 150 mM NaCl, 1 mM $CaCl_2$, and 0.5% glycerol and rapidly frozen in 2.5 μL aliquots at a concentration of 238 μM. Aliquots were thawed only once, immediately prior to use. S-Cnx was equilibrated at a final concentration of 9 μM in 20 mM Hepes at pH 7.4, 150 mM NaCl, and the indicated Ca^{2+} and/or ATP concentrations for 1 h at RT. FL was then diluted into the respective samples to a final concentration of 3 μM in a total volume of 150 μL. Aggregation was monitored immediately by measuring light scattering at 360 nm and 37 °C in a Shimadzu 1601 spectrophotometer equipped with a temperature-controlled sample compartment. Absorbance readings were taken every 6 s.

Fluorescence Experiments. S-Cnx (0.6 μM) was equilibrated in 150 μL of 20 mM Hepes at pH 7.4 and 150 mM NaCl at the indicated Ca^{2+} concentrations for 1 h at RT. Intrinsic fluorescence of S-Cnx was measured with an excitation wavelength of 280 nm. For measurements of the interaction between the hydrophobic fluorescent probe 1,1′-bis(4-anilino)naphthalene-5,5′-disulfonic acid (bis-ANS, Sigma) and S-Cnx, 1 μM S-Cnx was preincubated in 20 mM Hepes at pH 7.4 and 150 mM NaCl at the indicated Ca^{2+} or ATP concentrations for 1 h at RT. Subsequently bis-ANS was added to each sample to a final concentration of 6 μM. Bis-ANS fluorescence was monitored with an excitation wavelength of 395 nm. All fluorescence measurements were recorded at 37 °C using a Photon Technology International QM-1 fluorescence spectrofluorometer (excitation slit width: 2 nm; emission slit width: 5 nm).

Circular Dichroism Measurements. Unless otherwise indicated, S-Cnx (0.4 mg/mL) was preincubated in 150 μL of 20 mM Hepes at pH 7.4 and 150 mM NaCl at the indicated Ca^{2+} or ATP concentrations for 1 h at RT. Far-ultraviolet CD spectra were monitored using a Jasco J-810 spectropolarimeter from 200 to 260 nm in a 1 mm path length cuvette at 37 °C. The results are expressed as mean residue ellipticitiy [Θ] (λ) in units of deg·cm^2·dmol^{-1}, given by:

$$[\Theta](\lambda) = 100\,\frac{[\Theta](\lambda)}{c \cdot n \cdot l}$$

where Θ (λ) is the recorded ellipticity at wavelength λ in mdeg, c is the concentration in mM, n is the number of amino acid residues in S-Cnx, and l is the path length of the cuvette in cm. Thermal denaturation was measured by recording the change in ellipticity at 228 nm in the temperature range 20−80 °C using a scan rate of 2 °C/min. To determine the particular T_m values (transition midpoint temperature of thermal unfolding), the measured thermal denaturation curves were fit to a standard equation describing a two-state transition process by nonlinear least-squares regression using the software SigmaPlot 2004 version 9.0.

RESULTS

Effect of Ca^{2+} Concentration on the Aggregation Suppression Function of S-Cnx. To evaluate the lectin-independent aggregation function of S-Cnx at physiological temperature, we sought a substrate that would aggregate at 37 °C. Firefly luciferase (FL) is a thermolabile protein that is frequently used in vitro as a substrate in chaperone-mediated refolding or aggregation suppression assays, usually at temperatures greater than 37 °C or following dilution from a denaturant (*28*, *29*). It is also a non-glycosylated protein, and thus, any interaction with S-Cnx cannot be lectin-mediated. As shown in Figure 1A, FL in 20 mM Hepes buffer at pH 7.4 containing 150 mM NaCl aggregated at 37 °C following a lag period of 7−8 min. This behavior was unchanged in the presence of 1 mM Ca^{2+}. The addition of S-Cnx (3-fold molar excess) at the 1 mM Ca^{2+} concentration previously used in aggregation suppression assays involving S-Cnx or Crt (*21*, *22*) had only a small inhibitory effect on FL aggregation.

The Ca^{2+} concentration was then reduced to assess the potency of S-Cnx's aggregation suppression function under conditions that reflect the free ER Ca^{2+} store in its resting or filled state or following Ca^{2+} mobilization (empty state). Reducing the Ca^{2+} concentration resulted in a marked enhancement of the ability of S-Cnx to suppress FL aggregation (Figure 1A). Specifically, when Ca^{2+} was reduced to the 0.4 mM level reflective of the resting ER luminal Ca^{2+} concentration (*26*, *30*, *31*), S-Cnx inhibited the aggregation of FL by 55%. Furthermore, reduction of Ca^{2+} to the 50 μM level typically observed following mobilization of the ER Ca^{2+} store (*31*, *32*) completely suppressed FL aggregation. This aggregation suppression by S-Cnx was specific because the addition of a control protein, glutathione S-transferase (GST), in the absence of added Ca^{2+} had no effect on FL aggregation (Figure 1A).

Conformation of S-Cnx Is Influenced by Ca^{2+} Concentration. To understand the basis for the enhanced aggregation suppression function exhibited by S-Cnx as the Ca^{2+} concentration is reduced, the conformational consequences of altering the Ca^{2+} concentration were assessed using several approaches. Initially, we examined the far-UV circular dichroism (CD) spectrum of S-Cnx in the presence or absence of Ca^{2+}. As shown in Figure 1B, the CD spectrum of S-Cnx in the presence of 1 mM Ca^{2+} was characterized by a negative CD band at 228 nm but lacked secondary structure spectral features typical of proteins with a substantial content of β-sheets or α-helices. Rather, the spectrum appeared to be dominated by short wavelength aromatic CD transitions, which reflects the relatively high content of aromatic residues in the ER luminal domain of Cnx (9.5% of total residues). Similar observations have been made previously for Crt (*33*). No difference in the CD spectrum was observed upon reduction of the Ca^{2+} concentration to 0.4 mM, and only a minor decrease in mean residue ellipticity was associated with the complete absence of Ca^{2+}. However, the CD spectrum of S-Cnx denatured by heating at 80 °C was sufficiently distinct to permit an examination of the thermal stability of S-Cnx at various Ca^{2+} concentrations. The thermal denaturation curve of S-Cnx in 1 mM Ca^{2+} recorded at 228 nm shows that the protein denatures via a well-defined cooperative transition having a T_m of 49.5 °C (Figure 1C). This was unaltered when the Ca^{2+} concentration was reduced to the resting ER level of ~0.4 mM. However, further reduction led to a progressive loss of thermal stability such that at a Ca^{2+} concentration of 50 μM, typical of the empty ER, the T_m was reduced to 42.4 °C. These values resemble those reported for Crt at 1 mM Ca^{2+} (T_m = 46.4 °C) and at 50 μM Ca^{2+} (T_m = 44.3 °C) (*25*). Thus, Ca^{2+} ions have a stabilizing effect on both S-Cnx and Crt. We also made use of these Ca^{2+}-dependent changes in thermal stability to estimate the affinity of Ca^{2+} binding to S-Cnx, which has not been reported previously. As shown in Figure 1D, a plot of T_m versus Ca^{2+} concentration could be fit to an equation describing single site binding with a K_d = 125 μM.

We next examined the accessibility of S-Cnx to proteolytic digestion over a range of Ca^{2+} concentrations. Figure 2 shows that at 1 mM Ca^{2+} and at 37 °C, S-Cnx is relatively resistant to trypsin digestion with only slight shifts in electrophoretic mobility observed between 5 and 60 min of digestion. This has been observed previously and reflects clipping at both the N- and C-termini of ~68 kDa S-Cnx to give rise to a ~60 kDa protease-resistant core (*34*). No significant change was observed in the digestion pattern or kinetics when the

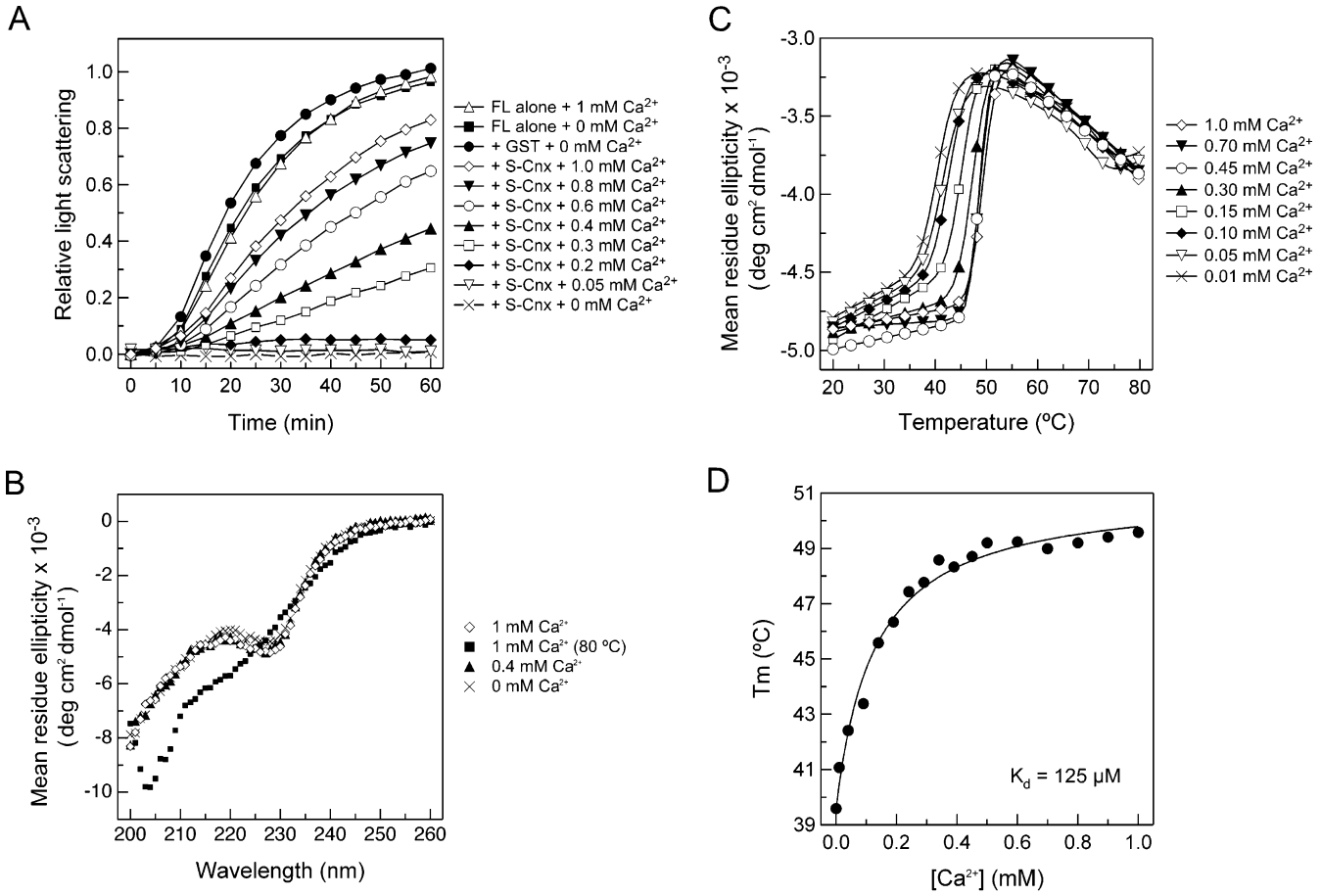

FIGURE 1: Ca^{2+} concentration influences the aggregation suppression function and the conformation of S-Cnx. (A) Effect of Ca^{2+} on the aggregation suppression function of S-Cnx. S-Cnx (or GST) (9 μM) was equilibrated in 20 mM Hepes at pH 7.4, 150 mM NaCl, and the indicated [Ca^{2+}] for 1 h at RT. FL was diluted into the various S-Cnx samples to a final concentration of 3 μM, and its aggregation was monitored by measuring light scattering at 360 nm and 37 °C. Data points were measured every 6 s and plotted every 5 min. (B) Far-UV CD spectra of S-Cnx. S-Cnx (0.1 mg/mL) was equilibrated in 5 mM Hepes at pH 7.4 and 150 mM NaCl with various concentrations of Ca^{2+} for 1 h at RT before recording the CD spectra (200−260 nm) at 37 or 80 °C. (C) Thermal stability of S-Cnx. S-Cnx (0.4 mg/mL) was equilibrated in 20 mM Hepes at pH 7.4, 150 mM NaCl, and the indicated Ca^{2+} concentrations for 1 h at RT. Thermal denaturation curves (20−80 °C) were obtained by measuring the mean residue ellipticity by CD at 228 nm. Data points were acquired every 2 °C but, for clarity, are shown every 5 °C. (D) Calculated T_m values of the thermal denaturation curves from panel C were plotted against [Ca^{2+}] and fit to an equation describing single site binding using SigmaPlot.

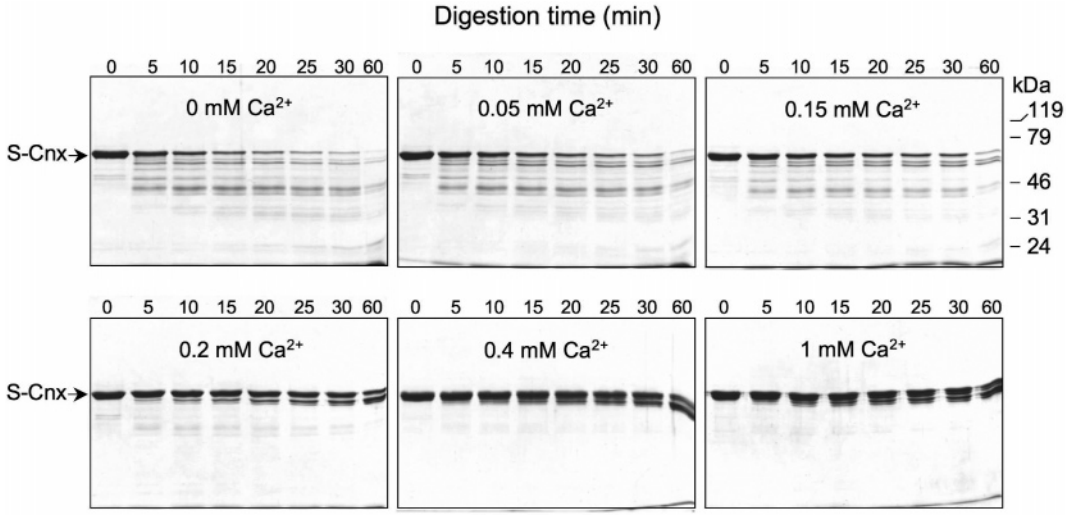

FIGURE 2: Protease sensitivity of S-Cnx. S-Cnx was preincubated in 20 mM Hepes at pH 7.4, 150 mM NaCl, and the indicated Ca^{2+} concentrations for 1 h at RT. All digestions were carried out at 37 °C with a S-Cnx/trypsin ratio of 100:1 (w/w). Aliquots containing 4 μg of S-Cnx were removed at each time point and analyzed by SDS−PAGE using 10% polyacrylamide gels followed by Coomassie Blue staining. The arrow indicates the S-Cnx band migrating at 68 kDa.

Ca^{2+} concentration was reduced to the resting ER level of 0.4 mM. However, further reduction in Ca^{2+} concentration led to a progressive increase in sensitivity to trypsin digestion, closely reflecting the loss of stability observed by CD

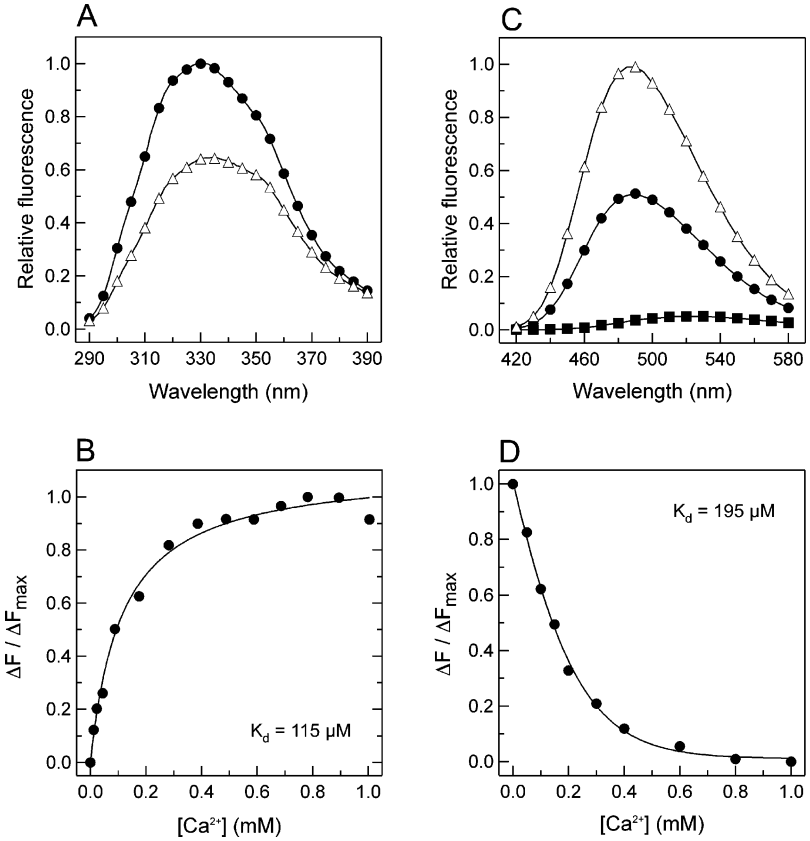

FIGURE 3: Influence of Ca^{2+} on intrinsic fluorescence and bis-ANS binding by S-Cnx. (A) Intrinsic fluorescence spectra of S-Cnx. S-Cnx (0.6 μM) was equilibrated in 20 mM Hepes at pH 7.4, 150 mM NaCl, and either 1 mM or 0 mM Ca^{2+} for 1 h at RT. The emission spectra (290−390 nm) were monitored at 37 °C with an excitation wavelength of 280 nm: (−●−) 1 mM Ca^{2+}; (−△−) 0 mM Ca^{2+}. Data points were measured every 1 nm and shown every 5 nm. (B) Intrinsic fluoresecence changes as a function of Ca^{2+} concentration. S-Cnx (0.6 μM) was preincubated in 20 mM Hepes at pH 7.4, 150 mM NaCl, and the indicated Ca^{2+} concentrations for 1 h at RT, and the intrinsic fluorescence was measured at 37 °C (excitation wavelength: 280 nm; emission wavelength: 333 nm). The results were plotted as the change in fluorescence (ΔF) divided by the maximum change in fluorescence between 1 and 0 mM Ca^{2+} (ΔF_{max}). The titration curve was fit to an equation describing single site binding using SigmaPlot. (C) Bis-ANS binding by S-Cnx. S-Cnx (1 μM) was equilibrated in 20 mM Hepes at pH 7.4, 150 mM NaCl in the presence or absence of 1 mM Ca^{2+} for 1h at RT and mixed with 6 μM bis-ANS. Bis-ANS fluorescence spectra were recorded between 420 and 580 nm at 37 °C with an excitation wavelength of 395 nm: (−■−) bis-ANS in 1 mM Ca^{2+}; (−●−) bis-ANS + S-Cnx + 1 mM Ca^{2+}; (−△−) bis-ANS + S-Cnx + 0 mM Ca^{2+}. Data points were measured every 1 nm and shown every 10 nm. (D) Bis-ANS fluoresecence changes as a function of Ca^{2+} concentration. S-Cnx (1 μM) was preincubated in 20 mM Hepes at pH 7.4, 150 mM NaCl, and the indicated Ca^{2+} concentrations for 1 h at RT before the addition of 6 μM bis-ANS. Bis-ANS fluorescence was measured at 37 °C (excitation wavelength: 395 nm; emission wavelength: 490 nm). The results were plotted as the change in fluorescence (ΔF) divided by the maximum change in fluorescence between 0 and 1 mM Ca^{2+} (ΔF_{max}). The data were fit to an equation describing single site binding using SigmaPlot.

spectroscopy (compare Figure 2 with Figure 1D). These findings are consistent with the loss of a tightly folded conformation of S-Cnx at Ca^{2+} concentrations below that of the resting ER.

Changes in the intrinsic (predominantly tryptophan) fluorescent emission spectrum of S-Cnx were also measured as a means to assess the nature of conformational changes in response to reductions in Ca^{2+} concentration. As illustrated in Figure 3A, the complete removal of Ca^{2+} ions from S-Cnx resulted in a major reduction in fluorescence emission intensity along with a shift of the spectrum to longer wavelengths. This is indicative of the transfer of one or more of the 13 tryptophan residues of S-Cnx from a hydrophobic environment to one that is more polar, probably exposed to solvent. Upon repeating this experiment at a variety of Ca^{2+} concentrations, it was observed that little change in the fluorescence emission intensity occurred upon lowering Ca^{2+} to the level of the resting ER (0.4 mM), but progressive quenching of fluorescence occurred at lower Ca^{2+} concentrations (Figure 3B). Fitting these data to a single site-binding model resulted in a K_d for Ca^{2+} binding to S-Cnx of 115 μM, quite similar to the K_d determined by measuring thermal stability as a function of Ca^{2+} concentration (Figure 1D).

Finally, binding of the hydrophobic fluorescent probe 1,1′-bis(4-anilino)naphthalene-5,5′-disulfonic acid (bis-ANS) was monitored as a measure of the surface hydrophobicity of S-Cnx. As shown in Figure 3C, when the emission spectra of bis-ANS alone or in the presence of S-Cnx (1 mM Ca^{2+}) were compared, bis-ANS exhibited the increase in fluorescence and the shift to shorter wavelength expected for its transfer from water to a hydrophobic environment. This confirms previous observations that S-Cnx at 1 mM Ca^{2+} possesses significant surface hydrophobicity (*21*). Upon the complete removal of Ca^{2+}, a further increase in bis-ANS fluorescence was observed, indicative of the increased exposure of hydrophobic sites (Figure 3C). Again, only a small portion of this Ca^{2+}-dependent hydrophobic exposure occurred when Ca^{2+} was reduced to the level of the resting ER (0.4 mM) with progressively more exposure resulting from further decreases in Ca^{2+} concentration (Figure 3D).

These data could be fit to a single site equation for Ca^{2+} binding with a $K_d = 195$ μM, in good agreement with the values obtained by CD and intrinsic fluorescence changes (Figure 3D).

Collectively, these assessments of S-Cnx conformation are consistent with a minor structural change associated with increased surface hydrophobicity when the Ca^{2+} concentration is reduced to the resting ER level. Further reductions in Ca^{2+} concentration are associated with a loss of stability and a less tightly packed conformation with likely exposure of the hydrophobic core.

Effect of Nucleotides on the Structure and Aggregation Suppression Function of S-Cnx. We showed previously that 1 mM ATP has a modest enhancing effect on the ability of S-Cnx to suppress the aggregation of citrate synthase at 45 °C (*21*). Figure 4A shows that this is also true for the suppression of FL aggregation at 37 °C in the presence of 1 mM Ca^{2+}. Furthermore, 2 mM ATP enhanced aggregation suppression by S-CNX even more, and in the presence of 3 mM ATP, the aggregation of FL was completely suppressed. We considered the possibility that these effects might be indirect because of a substantial drop in free Ca^{2+} concentration through chelation to the added nucleotide. However, direct measurement of free Ca^{2+} (see Experimental Procedures) revealed that the addition of 1 and 3 mM ATP reduced the free Ca^{2+} concentration from 1 to 0.9 and 0.7 mM, respectively. As shown in Figure 1A, such reductions in Ca^{2+} concentration are associated with only slight enhancements in the aggregation suppression function of S-Cnx (relative to 1 mM Ca^{2+}). We also considered that the reduced aggregation observed upon addition of ATP might be due to its binding to and stabilization of FL. However, 3 mM ATP had only minimal effects on FL aggregation when added in the absence of S-CNX (not shown) or in the presence of GST (Figure 4A). The addition of 1 mM Mg^{2+} did not influence the effect of ATP on the aggregation suppression function of S-CNX nor did it alter the outcome of subsequent conformational studies (data not shown).

To determine the structural basis for the enhanced aggregation suppression by S-CNX in the presence of ATP, far-UV CD spectra for S-CNX were collected at various ATP concentrations. As was the case for Ca^{2+}, only minimal changes in the spectra were observed (data not shown). Consequently, CD was used to monitor the thermal stability of S-CNX as a function of ATP concentration. As shown in Figure 4B, the addition of up to 3 mM ATP had little effect on S-CNX stability. The melting temperature decreased only 1 °C over the range of 0.5−3 mM ATP. Similarly, no alteration in S-CNX conformation in response to ATP could be detected by proteolytic digestion. Figure 4C shows that S-CNX remained largely resistant to digestion by trypsin at 37 °C (1 mM Ca^{2+}) either in the absence or presence of 5 mM ATP. However, a substantial increase in bis-ANS fluorescence was observed upon addition of ATP (Figure 5A). This was detectable at 0.5 mM ATP and reached a maximum near 5 mM ATP (Figure 5B). These data could be fit to a single site-binding model with a K_d for ATP binding to S-CNX of 2.9 mM. The marked increase in bis-ANS fluorescence coupled with the minimal changes in thermal stability and protease sensitivity are consistent with ATP inducing the exposure of a localized hydrophobic site on S-CNX.

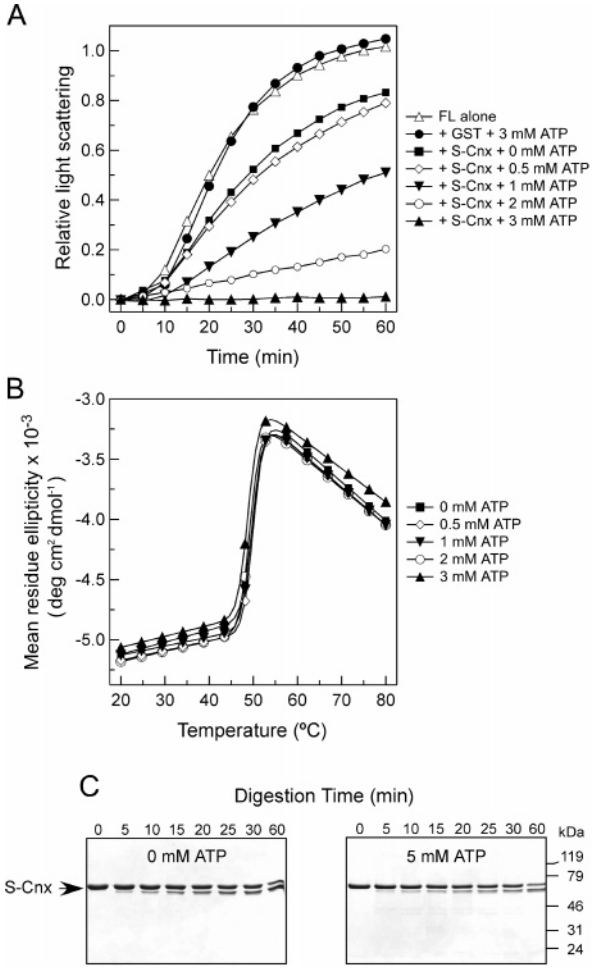

FIGURE 4: Effect of ATP on the structure and aggregation suppression function of S-Cnx. (A) ATP enhances the aggregation suppression function of S-Cnx. Following equilibration of S-Cnx or GST (9 μM) for 1 h at RT in 20 mM Hepes at pH 7.4, 150 mM NaCl, 1 mM $CaCl_2$, and the indicated ATP concentrations, 3 μM FL was added, and aggregation was monitored at 37 °C by light scattering at 360 nm. Data points were measured every 6 s but, for clarity, are shown every 5 min. (B) Effect of ATP on the thermal stability of S-Cnx. S-Cnx (0.4 mg/mL) was equilibrated in 20 mM Hepes at pH 7.4, 150 mM NaCl, 1 mM $CaCl_2$, and the indicated ATP concentrations for 1 h at RT. Thermal denaturation curves were recorded by measuring mean residue ellipticity by CD at 228 nm as the temperature was increased from 20 to 80 °C. Data points were measured every 2 °C and shown every 5 °C. (C) Influence of ATP on the trypsin susceptibility of S-Cnx. S-Cnx was incubated in 20 mM Hepes at pH 7.4, 150 mM NaCl, and 1 mM $CaCl_2$ in the presence or absence of 5 mM ATP for 1 h at RT. Digestions were performed at 37 °C using a S-Cnx/trypsin ratio of 100:1 (w/w), and aliquots containing 4 μg of S-Cnx were taken at the indicated time points. Digestion products were separated by SDS−PAGE using 10% polyacrylamide gels with visualization by Coomassie Blue staining. The arrow indicates the 68-kDa band of S-Cnx.

An examination of nucleotide specificity revealed that ATP was substantially more potent than either ADP or AMP in enhancing the aggregation suppression function of S-CNX (Figure 5C). In contrast, GTP was almost as potent as ATP, although this is unlikely to be physiologically relevant because there is no detectable GTP transporter activity within ER membranes (*35*). The ability of S-CNX to bind all of these nucleotides has been documented previously (*34*). Consistent with their effects on aggregation suppression, the addition of GTP to S-CNX increased bis-ANS fluorescence

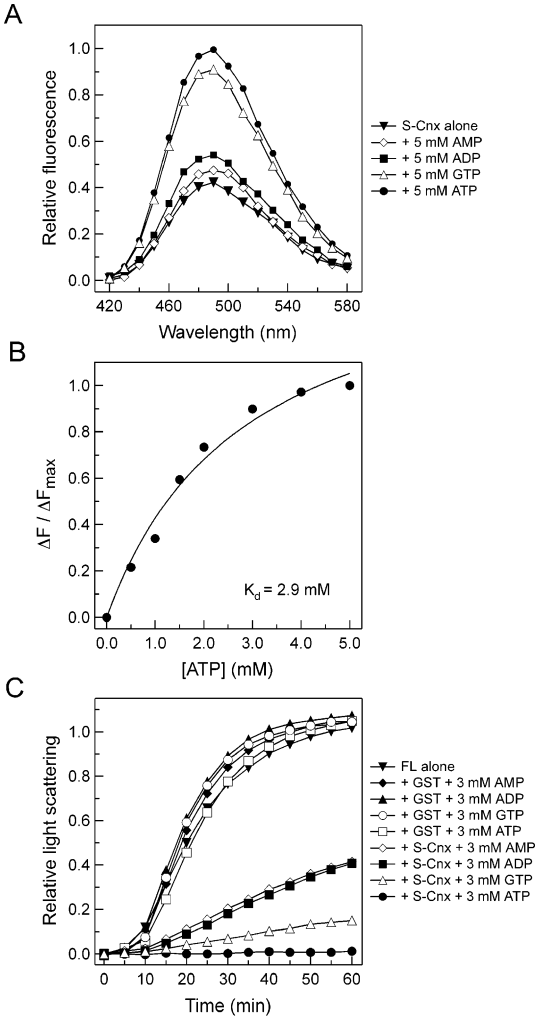

FIGURE 5: Influence of nucleotides on aggregation suppression and bis-ANS binding by S-Cnx. (A) Bis-ANS fluorescence. S-Cnx (1 μM) was equilibrated in 20 mM Hepes at pH 7.4, 150 mM NaCl, 1 mM $CaCl_2$, and 5 mM of the indicated nucleotides for 1 h at RT and then mixed with 6 μM bis-ANS. Bis-ANS fluorescence spectra (420−580 nm) were monitored with an excitation wavelength of 395 nm at 37 °C. Data points were measured every 1 nm and shown every 10 nm. (B) Bis-ANS fluorescence as a function of ATP concentration. S-Cnx (1 μM) was preincubated in 20 mM Hepes at pH 7.4, 150 mM NaCl, and 1 mM $CaCl_2$ with various concentrations of ATP for 1 h at RT before the addition of 6 μM bis-ANS. Bis-ANS fluorescence was measured at 37 °C with excitation and emission wavelengths of 395 and 490 nm, respectively. The results were plotted as the change in fluorescence (ΔF) divided by the maximum change in fluorescence between 0 and 5 mM ATP (ΔF_{max}). The titration curve was fit to an equation describing single site binding using SigmaPlot. (C) Effect of ATP on the aggregation suppression function of S-Cnx. S-Cnx (9 μM) was equilibrated in 20 mM Hepes at pH 7.4, 150 mM NaCl, 1 mM $CaCl_2$, and 3 mM of the indicated nucleotides for 1 h at RT. FL (3 μM) was pipetted into the various S-Cnx samples, and light scattering measurements were recorded at 360 nm at 37 °C. For clarity, data points were measured every 6 s but are plotted at 5 min intervals.

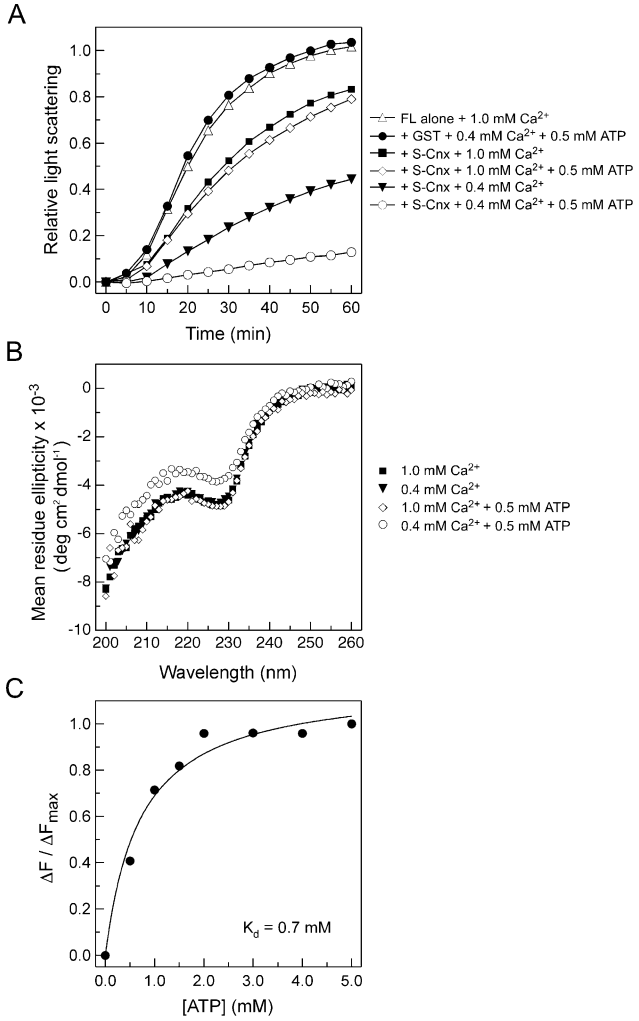

FIGURE 6: Synergistic effects of Ca^{2+} and ATP on the structure and aggregation suppression function of S-Cnx. (A) Suppression of FL aggregation. S-Cnx (9 μM) was equilibrated in 20 mM Hepes at pH 7.4, 150 mM NaCl, and the indicated Ca^{2+} and ATP concentrations for 1 h at RT. FL was added to the various S-Cnx samples at a final concentration of 3 μM, and its aggregation at 37 °C was monitored by measuring light scattering at 360 nm. Data points were measured every 6 s and shown every 5 min. (B) Far-UV CD spectra of S-Cnx. S-Cnx (0.1 mg/mL) was equilibrated in 5 mM Hepes at pH 7.4, 150 mM NaCl, and various concentrations of Ca^{2+} and ATP for 1 h at RT. CD spectra were recorded from 200 to 260 nm at 37 °C. (C) Bis-ANS binding to S-Cnx. S-Cnx (1 μM) was preincubated in 20 mM Hepes at pH 7.4, 150 mM NaCl, 0.4 mM Ca^{2+}, and the indicated ATP concentrations for 1 h at RT and mixed with 6 μM bis-ANS. Bis-ANS fluorescence was measured at 37 °C with excitation and emission wavelengths of 395 and 490 nm, respectively. The results were plotted as the change in fluorescence (ΔF) divided by the maximum change in fluorescence between 0 and 5 mM ATP (ΔF_{max}). The data were fit to an equation describing single site binding using SigmaPlot.

emission to almost the same extent as ATP, whereas ADP and AMP had only modest effects (Figure 5A). Thus, there is a direct correlation between nucleotide-regulated increases in surface hydrophobicity and the capacity of S-CNX to suppress FL aggregation.

Resting ER Ca^{2+} Concentration Potentiates the Effect of ATP on the Aggregation Suppression Function of S-Cnx. Because the lowering of Ca^{2+} concentration to the normal ER luminal level and the addition of 1−3 mM ATP independently enhanced the aggregation suppression function of S-Cnx, it was of interest to examine the combined effects of these treatments. As shown in Figure 6A, the addition of S-Cnx in the presence of 1 mM Ca^{2+} caused a modest suppression of FL aggregation. This was only slightly enhanced by the addition of 0.5 mM ATP (compare + S-Cnx + 1 mM Ca^{2+} and + S-Cnx + 1 mM Ca^{2+} + 0.5 mM ATP traces). Lowering the Ca^{2+} concentration to 0.4 mM in the absence of ATP substantially increased the potency of

aggregation suppression, as was observed previously (Figure 1A). However, in contrast to the situation at 1 mM Ca^{2+}, the addition of 0.5 mM ATP strongly potentiated aggregation suppression such that only a small degree of FL aggregation occurred (Figure 6A; compare + S-Cnx + 0.4 mM Ca^{2+} and + S-Cnx + 0.4 mM Ca^{2+} + 0.5 mM ATP traces). It appears that the reduction in Ca^{2+} concentration and the addition of ATP act synergistically to enhance the aggregation suppression function of S-Cnx. Again, this was not an indirect effect of ATP chelating Ca^{2+} because the direct measurement of free Ca^{2+} revealed that its concentration was reduced only slightly from 0.4 to 0.36 mM in the presence of 0.5 mM ATP. Furthermore, the effects were not due to altered FL stability because the addition of GST in the presence of 0.4 mM Ca^{2+} and 0.5 mM ATP did not alter the extent or kinetics of FL aggregation (Figure 6A).

Far-UV CD spectra revealed no significant differences between S-Cnx in the presence of either 1 mM Ca^{2+}, 0.4 mM Ca^{2+}, or 1 mM Ca^{2+}+ 0.5 mM ATP (Figure 6B). However, in the presence of 0.4 mM Ca^{2+}+ 0.5 mM ATP, a significant decrease in mean residue ellipticity was observed, consistent with conformational changes in the chaperone. These changes were not associated with a decrease in thermal stability or an increase in protease susceptibility (data not shown). Rather, an increase in the affinity of ATP binding to S-Cnx was observed. Whereas the K_d for ATP binding was 2.9 mM in the presence of 1 mM Ca^{2+} (Figure 5B), it decreased to 0.7 mM in the presence of 0.4 mM Ca^{2+}(Figure 6C), both assessed by monitoring ATP-associated changes in bis-ANS fluorescence emission. Thus, the resting ER luminal Ca^{2+} concentration of 0.4 mM exerts a significant impact on the ATP binding site of S-Cnx, lowering the ATP concentration required to trigger exposure of a hydrophobic site that appears to be involved in suppressing the aggregation of non-glycosylated polypeptide substrates.

DISCUSSION

In an effort to test the capacity of S-Cnx to suppress the aggregation of a non-glycosylated protein under physiological conditions of the ER lumen, several novel insights were obtained. First, S-Cnx is fully capable of suppressing the aggregation of thermally denatured FL through lectin-independent interactions at 37 °C. Therefore, this is an intrinsic property of S-Cnx and not merely a consequence of thermally induced unfolding of S-Cnx at the 43−45 °C temperatures used in previous studies with citrate synthase or malate dehydrogenase as substrates (*5*, *21*, *36*). In fact, in the present study, no evidence for thermally induced conformational changes in S-Cnx could be detected by CD at temperatures from 20 °C up to 45 °C (Figure 1C; 1 mM Ca^{2+}). Second, the aggregation suppression function of S-Cnx at 37 °C is influenced by Ca^{2+} concentration. Whereas most previous studies employed Ca^{2+} concentrations in the range of 1−2 mM (*21*, *24*), it was observed that aggregation suppression is significantly enhanced at the 0.4 mM concentration typical of the resting ER lumen and further enhanced at lower concentrations. Third, millimolar concentrations of ATP strongly potentiate aggregation suppression by S-Cnx, apparently through regulating the exposure of a hydrophobic binding site. Finally, lowering the Ca^{2+} concentration to resting levels increases the affinity of ATP binding to S-Cnx such that potent aggregation suppression can be effected under conditions likely to prevail within the lumen of the resting ER.

The importance of Ca^{2+} in maintaining the structural integrity of both S-Cnx and Crt has been well documented. Crt possesses a single high affinity Ca^{2+} binding site (K_d = 11 μM) and as many as 17 low affinity sites (K_d = 2 mM) (*37*). In the case of S-Cnx, the crystal structure revealed a single binding site for Ca^{2+} (*4*). Presumably, it is this site that we show in the present study that binds Ca^{2+} with a K_d = 0.1−0.2 mM. For both chaperones, complete chelation of Ca^{2+} results in a marked increase in protease susceptibility ((*25*, *34*, *38*) and Figure 2) and a loss of lectin function (*10*). Furthermore, the removal of Ca^{2+} results in destabilization of Crt with a decrease in melting temperature from 46.4 to 40.2 °C (*25*). We show a similar destabilization for S-Cnx in the absence of Ca^{2+}, with a decrease in melting temperature from 49.5 to 39.5 °C (Figure 1D). This was accompanied by a quenching of tryptophan fluorescence and an increase in hydrophobic exposure as measured by bis-ANS binding (Figure 3). Collectively, these findings are indicative of a loss of native structure for both S-Cnx and Crt upon Ca^{2+} removal, with an increase in conformational flexibility and likely exposure of the hydrophobic core. In contrast, the reduction of Ca^{2+} to the 0.4 mM level typical of the resting ER had barely detectable conformational consequences on S-Cnx. Compared to 1 mM Ca^{2+}, there was no discernible change in thermal stability or susceptibility to protease digestion. Only a slight quenching of intrinsic fluorescence and increase in surface hydrophobicity could be detected (Figure 3). Nevertheless, a substantial enhancement of the ability of S-Cnx to suppress the aggregation of FL was observed as the Ca^{2+} concentration was reduced from 1.0 to 0.4 mM (Figure 1A). These findings support the view that the aggregation suppression function of S-Cnx is associated with the native conformations it is likely to assume within the lumen of the resting ER.

The relevance of lower Ca^{2+} concentrations to Cnx function is less clear. Although the ability of S-Cnx to suppress FL aggregation increases continuously as Ca^{2+} is reduced from 0.4 mM down to the 50 μM level typical of the empty ER (Figure 1A), the associated loss of native structure and likely exposure of the hydrophobic interior suggest that the increased aggregation suppression may merely be a consequence of interactions arising from such exposure. Are low Ca^{2+}-induced structural changes in S-Cnx and enhanced interactions with folding glycoproteins likely to occur under physiological conditions? Most studies examining stimulus-induced changes in intracellular Ca^{2+} utilize Ca^{2+}-free medium or SERCA pump blockers to facilitate the detection of changes in ER Ca^{2+} levels (*26*). Under such conditions, reductions in free ER Ca^{2+} from 0.3 to 0.5 mM to 50 to 100 μM are commonly observed with ~30 s required to empty or refill ER stores. This suggests that there is ample opportunity for Cnx to undergo low Ca^{2+}-induced structural changes because we have observed in vitro that only a few seconds are required to completely dissociate Ca^{2+} from this chaperone (data not shown). However, recent experiments examining sarcoplasmic reticulum Ca^{2+} dynamics during muscle contraction in living mice have shown that Ca^{2+} levels fall by only 50 μM following nerve stimulation or by ~100 μM following combined nerve and β-adrenergic

stimulation. Also, cycles of Ca^{2+} release and recovery are extremely fast, on the order of 0.1 s (*39*). It is unlikely that such transient and modest fluctuations would have substantial impact on Cnx structure. However, until more in vivo experiments are performed on a variety of cell types under normal and pathological situations, the potential regulatory impacts of ER Ca^{2+} on Cnx structure remains an open question.

The ability of both S-Cnx and Crt to bind ATP is well established, although neither chaperone possesses ATPase activity (*21*, *22*, *34*, *38*). Using photo cross-linking, Ou et al. demonstrated the binding of ATP, ADP, AMP, and GTP to S-Cnx and the fact that these interactions require Mg^{2+} (*34*). They also reported an increased sensitivity to protease digestion in the presence of ATP, although we were unable to reproduce this finding previously (*10*). In the present study, we found that ATP is capable of binding to S-Cnx in the presence of 1 mM Ca^{2+} with a $K_d = 2.9$ mM and that this interaction does not require Mg^{2+} ions. It is not clear what form of ATP is binding to S-CNX in our experiments, but given the dissociation constants for metal binding to ATP (*40*, *41*) and the composition of the buffers used, Ca-ATP, Na-ATP, and free ATP are all candidates. Whatever the form of ATP that binds, it had no significant impact on the thermal stability of S-Cnx or in its maintenance of a tightly folded conformation. Rather, it was associated with a substantial increase in surface hydrophobicity, an effect that correlated with a strong potentiation in the ability of S-Cnx to suppress FL aggregation. These findings suggest that ATP binding regulates the exposure of a localized hydrophobic polypeptide binding site on S-Cnx. Remarkably, ATP binding affinity was increased 4-fold to a K_d of 0.7 mM when Ca^{2+} was reduced to the luminal ER concentration of 0.4 mM. This reduced the concentration of ATP required to obtain the suppression of FL aggregation such that near maximal suppression could be achieved at 0.5 mM rather than 2 mM ATP. Although this appears to be a very high effective concentration of ATP, it is likely that the ER lumen contains ATP in the millimolar range similar to that of the cytosol. ER membranes contain a robust ATP transporter (*35*), and several ER proteins are known ATPases, including the chaperones BiP and Grp94. It is noteworthy that Grp94 also exhibits very weak ATP binding (*42*, *43*) with a K_d likely to be in the 0.1−0.5 mM range[2], as observed for its cytosolic homologue, Hsp90 (*44*, *45*). Collectively, these findings suggest that S-Cnx is a highly effective chaperone capable of suppressing substrate aggregation through non-lectin interactions under conditions prevalent in the ER. They also suggest that under various stress conditions when ATP levels fall (*46*), the efficacy of Cnx in suppressing glycoprotein aggregation may be reduced. This could be a contributing factor to the induction of the ER unfolded protein response (*47*).

There is now substantial evidence that Cnx and Crt interact with at least some folding glycoproteins through polypeptide-based interactions in living cells. For example, although the prevention of lectin−oligosaccharide interactions with glucosidase inhibitors or in glucosidase-deficient cells prevents the formation of complexes between Cnx/Crt and some glycoproteins, such complexes are reduced in abundance or unaffected in the case of other glycoproteins (for a detailed list see ref 48 (*48*)). Presumably, various glycoproteins differ in the extent to which they associate with Cnx/Crt through lectin-based interactions alone or through combined lectin- and polypeptide-based interactions. Furthermore, we demonstrated that a lectin-deficient point mutant of Cnx remained fully capable of associating with class I histocompatibility molecules and delaying their unfolding/degradation when coexpressed in cells (*49*). Conversely, lectin-competent Cnx associates perfectly well with completely non-glycosylated class I histocompatibility molecules (*48*). Also, the recent demonstration that Cnx remains bound to the misfolded VSV G glycoprotein for as long as 60 min in the absence of a reglucosylation cycle raises the question of how this might occur if mediated solely through a demonstrably weak lectin−oligosaccharide interaction (*50*, *51*).

How can polypeptide-based interactions be integrated into a functional chaperone cycle for Cnx, especially in light of an apparent ATP-regulated binding site? Regulation of substrate binding by ATP is a common feature of chaperones of the Hsp60, Hsp70, and Hsp90 classes (*52*), although only Hsp90 shares with S-Cnx the property of increased substrate interaction in the presence of ATP (*53*). Furthermore, these classical chaperones all possess varying degrees of ATPase activity that is essential for a functional binding-release cycle. Cnx, however, lacks ATPase activity (*21*), and thus, it is likely that the weak affinity of this chaperone for ATP coupled with a high ER luminal ATP concentration ensures that Cnx is in equilibrium between ATP-occupied and ATP-unoccupied states. Therefore, in conjunction with cyclic lectin interactions, Cnx could cycle between an ATP-bound state with high affinity for unfolded polypeptides and a lower affinity ATP-unbound state. It will be of interest to test this concept by reconstituting functional Cnx cycles in the refolding of non-glycosylated or monoglucosylated substrates and assessing the regulatory effects of various ATP concentrations.

[2] Christopher Nicchitta, personal communication.

ACKNOWLEDGMENT

We thank David Isenman and Reinhart Reithmeier for helpful discussions and the critical reading of this manuscript. We also thank Myrna Cohen-Doyle for technical assistance, Cosmin Pocanschi for advice, Ronnie Lum and Johnny Tkach for reagents, and Reinhold Vieth and Man Khun Chan for calcium concentration measurements.

REFERENCES

1. Hebert, D. N., Garman, S. C., and Molinari, M. (2005) The glycan code of the endoplasmic reticulum: asparagine-linked carbohydrates as protein maturation and quality-control tags, *Trends Cell Biol. 15*, 364−370.
2. Helenius, A., and Aebi, M. (2004) Roles of N-linked glycans in the endoplasmic reticulum, *Annu. Rev. Biochem. 73*, 1019−1049.
3. Williams, D. B. (2006) Beyond lectins: the calnexin/calreticulin chaperone system of the endoplasmic reticulum, *J. Cell Sci. 119*, 615−623.
4. Schrag, J. D., Bergeron, J. J., Li, Y., Borisova, S., Hahn, M., Thomas, D. Y., and Cygler, M. (2001) The structure of calnexin, an ER chaperone involved in quality control of protein folding, *Mol. Cell 8*, 633−644.
5. Leach, M. R., Cohen-Doyle, M. F., Thomas, D. Y., and Williams, D. B. (2002) Localization of the lectin, ERp57 binding, and polypeptide binding sites of calnexin and calreticulin, *J. Biol. Chem. 277*, 29686−29697.

6. Ware, F. E., Vassilakos, A., Peterson, P. A., Jackson, M. R., Lehrman, M. A., and Williams, D. B. (1995) The molecular chaperone calnexin binds Glc1Man9GlcNAc2 oligosaccharide as an initial step in recognizing unfolded glycoproteins, *J. Biol. Chem. 270*, 4697−4704.
7. Pollock, S., Kozlov, G., Pelletier, M. F., Trempe, J. F., Jansen, G., Sitnikov, D., Bergeron, J. J., Gehring, K., Ekiel, I., and Thomas, D. Y. (2004) Specific interaction of ERp57 and calnexin determined by NMR spectroscopy and an ER two-hybrid system, *EMBO J. 23*, 1020−1029.
8. Frickel, E. M., Riek, R., Jelesarov, I., Helenius, A., Wuthrich, K., and Ellgaard, L. (2002) TROSY-NMR reveals interaction between ERp57 and the tip of the calreticulin P-domain, *Proc. Natl. Acad. Sci. U.S.A. 99*, 1954−1959.
9. Spiro, R. G., Zhu, Q., Bhoyroo, V., and Soling, H. D. (1996) Definition of the lectin-like properties of the molecular chaperone, calreticulin, and demonstration of its copurification with endomannosidase from rat liver Golgi, *J. Biol. Chem. 271*, 11588−11594.
10. Vassilakos, A., Michalak, M., Lehrman, M. A., and Williams, D. B. (1998) Oligosaccharide binding characteristics of the molecular chaperones calnexin and calreticulin, *Biochemistry 37*, 3480−3490.
11. Hammond, C., Braakman, I., and Helenius, A. (1994) Role of N-linked oligosaccharide recognition, glucose trimming, and calnexin in glycoprotein folding and quality control, *Proc. Natl. Acad. Sci. U.S.A. 91*, 913−917.
12. Hebert, D. N., Foellmer, B., and Helenius, A. (1995) Glucose trimming and reglucosylation determine glycoprotein association with calnexin in the endoplasmic reticulum, *Cell 81*, 425−433.
13. Caramelo, J. J., Castro, O. A., de Prat-Gay, G., and Parodi, A. J. (2004) The endoplasmic reticulum glucosyltransferase recognizes nearly native glycoprotein folding intermediates, *J. Biol. Chem. 279*, 46280−46285.
14. Ritter, C., Quirin, K., Kowarik, M., and Helenius, A. (2005) Minor folding defects trigger local modification of glycoproteins by the ER folding sensor GT, *EMBO J. 24*, 1730−1738.
15. Taylor, S. C., Ferguson, A. D., Bergeron, J. J., and Thomas, D. Y. (2004) The ER protein folding sensor UDP-glucose glycoprotein-glucosyltransferase modifies substrates distant to local changes in glycoprotein conformation, *Nat. Struct. Mol. Biol. 11*, 128−134.
16. High, S., Lecomte, F. J., Russell, S. J., Abell, B. M., and Oliver, J. D. (2000) Glycoprotein folding in the endoplasmic reticulum: a tale of three chaperones? *FEBS Lett. 476*, 38−41.
17. Jackson, M. R., Cohen-Doyle, M. F., Peterson, P. A., and Williams, D. B. (1994) Regulation of MHC class I transport by the molecular chaperone, calnexin (p88, IP90), *Science 263*, 384−387.
18. Molinari, M., Calanca, V., Galli, C., Lucca, P., and Paganetti, P. (2003) Role of EDEM in the release of misfolded glycoproteins from the calnexin cycle, *Science 299*, 1397−1400.
19. Oda, Y., Hosokawa, N., Wada, I., and Nagata, K. (2003) EDEM as an acceptor of terminally misfolded glycoproteins released from calnexin, *Science 299*, 1394−1397.
20. Rajagopalan, S., Xu, Y., and Brenner, M. B. (1994) Retention of unassembled components of integral membrane proteins by calnexin, *Science 263*, 387−390.
21. Ihara, Y., Cohen-Doyle, M. F., Saito, Y., and Williams, D. B. (1999) Calnexin discriminates between protein conformational states and functions as a molecular chaperone in vitro, *Mol. Cell. 4*, 331−341.
22. Saito, Y., Ihara, Y., Leach, M. R., Cohen-Doyle, M. F., and Williams, D. B. (1999) Calreticulin functions in vitro as a molecular chaperone for both glycosylated and non-glycosylated proteins, *EMBO J. 18*, 6718−6729.
23. Rizvi, S. M., Mancino, L., Thammavongsa, V., Cantley, R. L., and Raghavan, M. (2004) A polypeptide binding conformation of calreticulin is induced by heat shock, calcium depletion, or by deletion of the C-terminal acidic region, *Mol. Cell. 15*, 913−923.
24. Thammavongsa, V., Mancino, L., and Raghavan, M. (2005) Polypeptide substrate recognition by calnexin requires specific conformations of the calnexin protein, *J. Biol. Chem. 280*, 33497−33505.
25. Li, Z., Stafford, W. F., and Bouvier, M. (2001) The metal ion binding properties of calreticulin modulate its conformational flexibility and thermal stability, *Biochemistry 40*, 11193−11201.
26. Meldolesi, J., and Pozzan, T. (1998) The endoplasmic reticulum Ca2+ store: a view from the lumen, *Trends Biochem. Sci. 23*, 10−14.
27. Bessette, P. H., Aslund, F., Beckwith, J., and Georgiou, G. (1999) Efficient folding of proteins with multiple disulfide bonds in the Escherichia coli cytoplasm, *Proc. Natl. Acad. Sci. U.S.A. 96*, 13703−13708.
28. Kubo, Y., Tsunehiro, T., Nishikawa, S., Nakai, M., Ikeda, E., Toh-e, A., Morishima, N., Shibata, T., and Endo, T. (1999) Two distinct mechanisms operate in the reactivation of heat-denatured proteins by the mitochondrial Hsp70/Mdj1p/Yge1p chaperone system, *J. Mol. Biol. 286*, 447−464.
29. Szabo, A., Langer, T., Schroder, H., Flanagan, J., Bukau, B., and Hartl, F. U. (1994) The ATP hydrolysis-dependent reaction cycle of the Escherichia coli Hsp70 system DnaK, DnaJ, and GrpE, *Proc. Natl. Acad. Sci. U.S.A. 91*, 10345−10349.
30. Foyouzi-Youssefi, R., Arnaudeau, S., Borner, C., Kelley, W. L., Tschopp, J., Lew, D. P., Demaurex, N., and Krause, K. H. (2000) Bcl-2 decreases the free Ca2+ concentration within the endoplasmic reticulum, *Proc. Natl. Acad. Sci. U.S.A. 97*, 5723−5728.
31. Miyawaki, A., Llopis, J., Heim, R., McCaffery, J. M., Adams, J. A., Ikura, M., and Tsien, R. Y. (1997) Fluorescent indicators for Ca2+ based on green fluorescent proteins and calmodulin, *Nature 388*, 882−887.
32. Michalak, M., Parker, J. M. R., and Opas, M. (2002) Ca2+ signaling and calcium binding chaperones of the endoplasmic reticulum, *Cell Calcium 32*, 269−278.
33. Bouvier, M., and Stafford, W. F. (2000) Probing the three-dimensional structure of human calreticulin, *Biochemistry 39*, 14950−14959.
34. Ou, W. J., Bergeron, J. J., Li, Y., Kang, C. Y., and Thomas, D. Y. (1995) Conformational changes induced in the endoplasmic reticulum luminal domain of calnexin by Mg-ATP and Ca2+, *J. Biol. Chem. 270*, 18051−18059.
35. Guillen, E., and Hirschberg, C. B. (1995) Transport of adenosine triphosphate into endoplasmic reticulum proteoliposomes, *Biochemistry 34*, 5472−5476.
36. Stronge, V. S., Saito, Y., Ihara, Y., and Williams, D. B. (2001) Relationship between calnexin and BiP in suppressing aggregation and promoting refolding of protein and glycoprotein substrates, *J. Biol. Chem. 276*, 39779−397787.
37. Baksh, S., and Michalak, M. (1991) Expression of calreticulin in Escherichia coli and identification of its Ca2+ binding domains, *J. Biol. Chem. 266*, 21458−21465.
38. Corbett, E. F., Michalak, K. M., Oikawa, K., Johnson, S., Campbell, I. D., Eggleton, P., Kay, C., and Michalak, M. (2000) The conformation of calreticulin is influenced by the endoplasmic reticulum luminal environment, *J. Biol. Chem. 275*, 27177−27185.
39. Rudolf, R., Magalhaes, P. J., and Pozzan, T. (2006) Direct in vivo monitoring of sarcoplasmic reticulum Ca2+ and cytosolic cAMP dynamics in mouse skeletal muscle, *J. Cell Biol. 173*, 187−193.
40. Adolfsen, R., and Moudrianakis, E. N. (1978) Control of complex metal ion equilibria in biochemical reaction systems. Intrinsic and apparent stability constants of metal-adenine nucleotide complexes, *J. Biol. Chem. 253*, 4378−4379.
41. Graf, E., and Penniston, J. T. (1981) CaATP: the substrate, at low ATP concentrations, of Ca2+ ATPase from human erythrocyte membranes, *J. Biol. Chem. 256*, 1587−1592.
42. Csermely, P., Miyata, Y., Schnaider, T., and Yahara, I. (1995) Autophosphorylation of grp94 (endoplasmin), *J. Biol. Chem. 270*, 6381−6388.
43. Rosser, M. F., and Nicchitta, C. V. (2000) Ligand interactions in the adenosine nucleotide-binding domain of the Hsp90 chaperone, GRP94. I. Evidence for allosteric regulation of ligand binding, *J. Biol. Chem. 275*, 22798−22805.
44. Csermely, P., and Kahn, C. R. (1991) The 90-kDa heat shock protein (hsp-90) possesses an ATP binding site and autophosphorylating activity, *J. Biol. Chem. 266*, 4943−4950.
45. Scheibel, T., Neuhofen, S., Weikl, T., Mayr, C., Reinstein, J., Vogel, P. D., and Buchner, J. (1997) ATP-binding properties of human Hsp90, *J. Biol. Chem. 272*, 18608−18613.
46. Soti, C., Sreedhart, A. S., and Csermely, P. (2003) Apoptosis, necrosis and cellular senescence: chaperone occupancy as a potential switch, *Aging Cell 2*, 39−45.
47. Zhang, K., and Kaufman, R. J. (2006) The unfolded protein response: a stress signaling pathway critical for health and disease, *Neurology 66*, S102−S109.

48. Danilczyk, U. G., and Williams, D. B. (2001) The lectin chaperone calnexin utilizes polypeptide-based interactions to associate with many of its substrates in vivo, *J. Biol. Chem. 276*, 25532−25540.
49. Leach, M. R., and Williams, D. B. (2004) Lectin-deficient calnexin is capable of binding class I histocompatibility molecules in vivo and preventing their degradation, *J. Biol. Chem. 279*, 9072−9079.
50. Kapoor, M., Srinivas, H., Kandiah, E., Gemma, E., Ellgaard, L., Oscarson, S., Helenius, A., and Surolia, A. (2003) Interactions of substrate with calreticulin, an endoplasmic reticulum chaperone, *J. Biol. Chem. 278*, 6194−6200.
51. Molinari, M., Galli, C., Vanoni, O., Arnold, S. M., and Kaufman, R. J. (2005) Persistent glycoprotein misfolding activates the glucosidase II/UGT1-driven calnexin cycle to delay aggregation and loss of folding competence, *Mol. Cell. 20*, 503−512.
52. Young, J. C., Agashe, V. R., Siegers, K., and Hartl, F. U. (2004) Pathways of chaperone-mediated protein folding in the cytosol, *Nat. Rev. Mol. Cell Biol. 5*, 781−791.
53. Pearl, L. H., and Prodromou, C. (2006) Structure and mechanism of the hsp90 molecular chaperone machinery, *Annu. Rev. Biochem. 75*, 271−294.
54. Leach, M. R., and Williams, D. B. (2003) Calnexin and Calreticulin, Molecular Chaperones of the ER, in *Calreticulin*, (Michalak, M., and Eggleton, P., Eds.) 2nd ed., pp 49−62, Landes Bioscience, Georgetown, Texas.

BI0614378